Level of Detail Visual Analysis of Structures in Solid-State Materials

Signe Sidwall Thygesen, Alexei I. Abrikosov, Peter Steneteg, Talha Bin Masood, Ingrid Hotz

Scientific Visualization Group, Linköping University, Sweden

Abstract

We propose a visual analysis method for the comparison and evaluation of structures in solid-state materials based on the electron density field using topological analysis. The work has been motivated by a material science application, specifically looking for new so-called layered materials whose physical properties are required in many modern technological developments. Due to the incredibly large search space, this is a slow and tedious process, requiring efficient data analysis to characterize and understand the material properties. The core of our proposed analysis pipeline is an abstract bar representation that serves as a concise signature of the material, supporting direct comparison and also an exploration of different material candidates.

1. Introduction

This article presents a visual analysis tool developed in collaboration with physicists and has contributed to several physics publications [BFC*21,CTOL*21,LTY*23]. The application context is engineering novel materials with specific properties, an essential task for many technological advancements [CCK*14]. One class of materials gaining interest is "layered" materials, e.g., graphite [BB24]. Such materials are solids made up of weakly bonded layers of atoms, having interesting properties with many applications ranging from energy storage to biomedicine [Gut20]. Much effort is put into synthesis and simulation to find new materials with the desired properties. Due to a large number of possible candidates the search for suitable materials is a slow and tedious process that requires efficient data analysis to characterize and understand the material properties. Here we contribute with a novel visual analysis concept supporting an easy comparison of such data.

Our analysis focuses on the electron density, which is generally considered to be the most complete description of materials' properties [SMH*22] and is increasingly available in databases, e.g., the Materials Project [JOH*13]. However, despite its significance, it is seldom explored in full detail. This might be due to missing tools supporting direct comparison of electron density fields. The goal of this work is to explore in how a full analysis of the electron density can support the material exploration process. We focus on the development of feature descriptors that support quantitative and visually comparative analysis of the structure of the density field. Since topological data analysis provides a rich set of methods for this purpose [YMS*21] it forms the basis for our work.

Our work builds on standard topological descriptors such as the merge tree [YMS*21] to derive a concise signature of the material that aggregates the most important properties of the data in one view. For this purpose, we exploit the specific structure of the data, which is made up of relatively simple periodic unit cells, typically with less than about a hundred atoms. The saddle points often have a direct physical meaning. In layered materials, there are different types of saddle events: from atoms to bonds, to chains, to layers, and to one component which we summarize in a bar signature. Such bars can be placed next to each other for comparison and expanded on demand for detailed investigations. A link back to spatial representations, familiar to scientists, is also provided. Selecting a saddle point of interest automatically generates a transfer function highlighting the related changes in the field. We first demonstrate the usefulness of the method on the case that motivated this work, two further examples show the generality of the work.

Related work. Topological analysis of the electron density field has a long tradition in characterizing atomic interactions based on Bader's theory of *Atoms in Molecules* [Bad85]. Density values at bond critical points serve as indicators for the interaction strength [JKMS*10]. However, such methods are rarely used for data summarization and comparison. In visualization, topological analysis of electron density fields has mostly been using Morse-Smale decomposition of the domain [AMFH21]. Examples include the characterization of atomic bonds in molecular systems by Gunther et al. [GBCG*14], the exploration of molecular and condensed-matter systems by Bathia et al. [BGL*18], or a Morse-Smale analysis of ion diffusion in battery materials by Gyulassy et al. [GKL*15]. In general, tree visualization is a fundamental component in information visualization. A variety of layouts and interaction techniques have been developed, mostly targeting large and complex tree structures, summarized by Graham et al. [GK10]. Methods for comparing topological structures, including merge trees, can be found in the state-of-the-art report by Yan et al. [YMS*21]. An attempt to visually summarize a set of merging trees is the Lohfink et al. [LWL*20] fuzzy contour tree, which aims at general scalar fields. In contrast to this generic approach, we are interested in a specific class of scalar fields that can be exploited to obtain less complex representations. The automatic gen-

eration of transfer functions used in our work builds on ideas from the topology-driven volume rendering by Weber et al. [WDC*07].

2. Data

The considered data is electron density fields, from numerical simulations, given as a scalar field on a grid, together with the atomic positions of the material. All materials are periodic crystals. Two of our case studies are layered materials: beryllium tetranitride (BeN_4) [BFC*21] and nickel dinitride (NiN_2) [BBP*21], both have small unit cells with 5 atoms in the unit cell for BeN_4 and 6 atoms for NiN_2. BeN_4 is initially synthesized at high pressure and forms layers as the pressure is released to ambient conditions. Its electron density field is given at seven pressure points: 0, 6.8, 11.8, 17.8, 25.6, 40.5, and 83.6 GPa. The NiN_2 data is available for two different types: marcasite type m-NiN_2 and pentagonal type p-NiN_2. The p-NiN_2 is layered, whereas the m-NiN_2 is not layered. These two structures are compared at a single pressure of 38 GPa which is the formation pressure of m-NiN_2. The third case study compares a pure metal Niobium (Nb) and a high entropy alloy (HEA) consisting of a mix of five different metals Niobium, Hafnium (Hf), Zirconium (Zr), Titanium (Ti) and Vanadium (V) [CTOL*21]. The metal and alloy consist of 120 atoms. Thus, they have larger unit cells, which are needed to capture the disordered nature of the alloy. The periodicity is enforced by the simulation.

Data assumptions. The method's design builds on the following assumptions. (i) The data is periodic, given by a unit cell that expands in all directions. (ii) The unit cell is in the order of magnitude of a hundred atoms. (iii) Maxima in the scalar field represent atoms, and saddles represent bondings between atoms or atomic groups, according to Bader's theory of Atoms in Molecules [Bad85].

3. Method and Design

Task Analysis. To support the analysis of structures in solid-state materials we identify the following key tasks:

T1 Quantification of the structures in the material, based on the electron density field, represented in a *material descriptor.*

T2 Visualization of the material descriptor, suited for comparison between material configurations.

T3 Automatic visualization of the electron density field to inspect and verify found material structures.

Method overview. The *merge tree*, capturing the material's structure from the charge density fields, builds the center of our visualization and analysis method. To capture all structural events, it is computed from an expanded cell according to the periodic boundary conditions. We support the visualization of the full merge tree or collapsed summary bar that is better suited for comparison. To link this abstract visualization back to the charge density data, we use an isosurface visualization of the density with an automatically specified isovalue based on nodes of interest from the merge tree (Figure 2 (a)). The prototype is mainly implemented in Inviwo [JSS*19] which uses Topology Toolkit [TFL*17] for the topological analysis at the back-end and D3 [BOH11] for the interactive front-end.

3.1. Merge tree as a material descriptor (T1)

Given a scalar field $f : X \to \mathbb{R}$ defined on a connected space X, the *merge tree* keeps track of the connectivity of the super-level (or sub-

level) sets of f as the function value changes [CSA03, YMS*21]. The electron density field has maxima at the atom positions and decays with the distance from the atom. We are interested in capturing these maxima and how they merge together into different structures. Therefore, we use a version of the merge tree called *join tree* which tracks the super-level sets of f. Its leaves are the maxima of the scalar field, and its global minimum is the root. The tree branches are at saddle points where two super-level sets merge together. We use a small persistence threshold equivalent to 1% of the scalar field range to filter out topological noise from the trees.

Treatment of periodic boundary conditions. The periodic crystal structure is given by a small unit cell that infinitely repeats in all three spatial dimensions. If we compute the merge tree of the charge density field in a single unit cell without considering the periodic boundary conditions, we will obtain an incomplete topological picture of the density field. However, directly applying periodic boundary conditions to a single unit cell is not sufficient. Some important merge events occur between components that are identified through periodic boundaries, whereas they are different in the expanded infinite crystal lattice, see Figure 1. To address this issue, we instead compute the merge tree for an expanded $2 \times 2 \times 2$ cell with periodic boundaries. This ensures that all key structural changes in the infinite crystal lattice are captured in the merge tree.
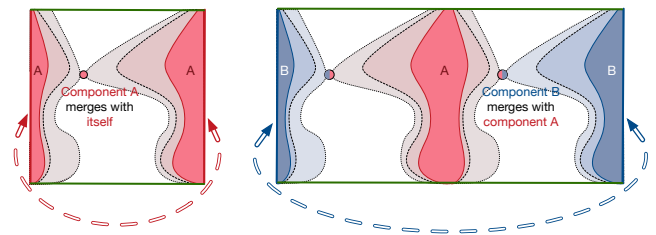

Figure 1: *Applying periodic boundary conditions. (left) the merge between the two components A will not be detected. (right) Creating an expanded cell, here in 1 dim, all merges are correctly tracked.*
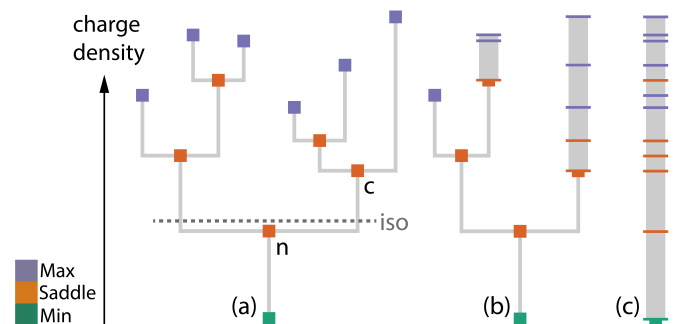

Figure 2: *Layout of the material descriptor: (a) Full tree, which can be collapsed interactively at each saddle-node summarizing its subtree into a bar, (b) partly collapsed tree, (c) fully collapsed tree. Each node in the tree is highlighted with a line at the corresponding node value, using distinct colors based on critical type. Automatic isovalue generation to highlight structural changes, based on the values in node n and closest child c is highlighted in (a).*
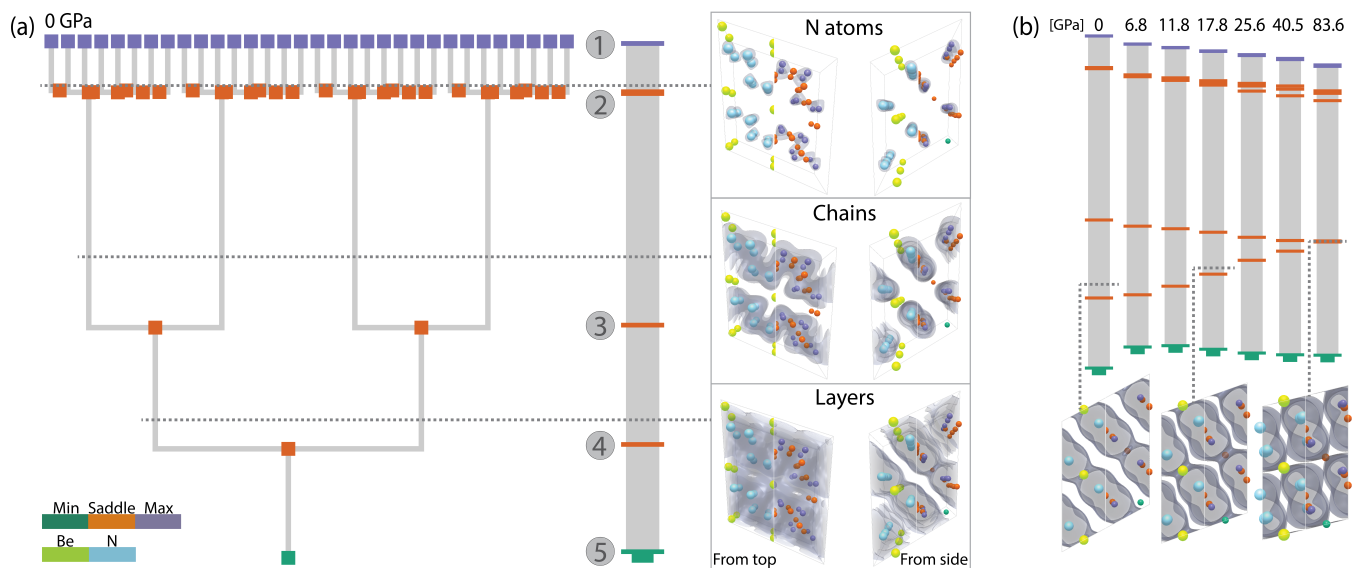
Figure 3: *(a) Visualization of the material descriptor for BeN$_4$ at pressure 0 GPa. Full tree and the summary bar, decreasing the charge density from high (leaves in the tree) to low captures the main types of events in the saddle-nodes: 1. The N atom-components are born at maxima, 2. They merge together with N-N bonds which then merge into chains, 3. The chains merge into layers, 4. The layers merge together, and finally 5. the single component dies at the global minimum. Isosurfaces for relevant saddle points, together with atoms and critical point positions, further highlight these structures (using perspective projection). (b) Summary bars for all seven pressures in comparison together with isosurfaces for the lowest saddle for the pressures: 0, 17.8, 83.6 GPa (using orthographic projection).*

3.2. Visualizing the material descriptor (T2)

The full material descriptor is the merge tree, which can be visualized directly. Its nodes are colored according to the type of the critical point (minima, saddle, maxima) using a qualitative color map (colorbrewer2.org). The root of the tree (the global minimum) is placed at the bottom and the leaf nodes (maxima) at the top. The height corresponds to the charge density value, with the possibility to use both linear and logarithmic scales, see Figure 2 (a). Since the full tree is not well suited for a comparison of multiple material structures, we design a summary bar as a collapsed version of the tree. The summary bar shows each node value as a line marked over a gray vertical bar. An example is shown in Figure 2 (b, c). By clicking a node, one can interactively collapse or expand the subtree rooted under that node. This gives the possibility to decide the amount of information to show on demand. The collapsed tree serves as a quick overview of the material structure. For comparison, the summary bars are aligned according to their density values.

3.3. Spatial visualization of the charge density (T3)

To inspect the structural changes at each node in the tree, we use an isosurface visualization providing a link to the charge density distribution in space to verify the structures highlighted in the merge tree. The direct value of a node in the tree gives us the exact point when a merge happens, to show the structure just before this merge we automatically specify a value slightly above the value in the selected saddle node n with value $f(n)$. To determine the isovalue for the rendering, we first find the child c in the subtree rooted at n with the lowest value $f(c)$. The isovalue is then specified as $iso = f(n) + 0.1(f(c) - f(n))$, see Figure 2 (a). We show the extracted isosurfaces in gray as a default. This allows for the possibility to highlight atom positions or critical point positions in color.

We choose either perspective or orthographic projection in the rendering process, depending on which highlights the structures best. The rendering can be augmented with spheres showing atomic positions, Atoms colored according to the CPK color convention. Alternatively, the saddle points highlighting the first merge of the individual components can be shown.

4. Case studies

We illustrate our method by applying it to simulated material data described earlier in section 2. First, we apply our method to the two types of layered materials. The final case study concerns the comparison of a pure metal to a metal alloy.

4.1. Layered materials

We first examine the full merge tree of BeN$_4$ for an expanded cell at pressure 0 GPa and inspect the isosurfaces together with the atom positions and critical point positions at different levels in the tree as proposed in subsection 3.3. In all images, we use a logarithmic scale for the charge density. We conclude the following essential events in Figure 3 (a): 1. The super-level set components are born at the maxima corresponding to the N atoms. 2. These components merge at the saddles corresponding to N−N bonds to form N−N bond chains. 3. The N−N bond chains merge to form layers. 4. All the layers then merge into a single connected component. 5. Finally, the single component dies at the global minimum. The merge trees for the other pressures show a similar structure, but with a gradual change in critical point values, as illustrated in the summary bars in Figure 3 (b). An important observation is the change in values for the saddle points corresponding to the layer merge and chain merge (the bottom two saddle nodes in the summary bar). For pressure 0 GPa these two nodes have a clear separation, meaning this
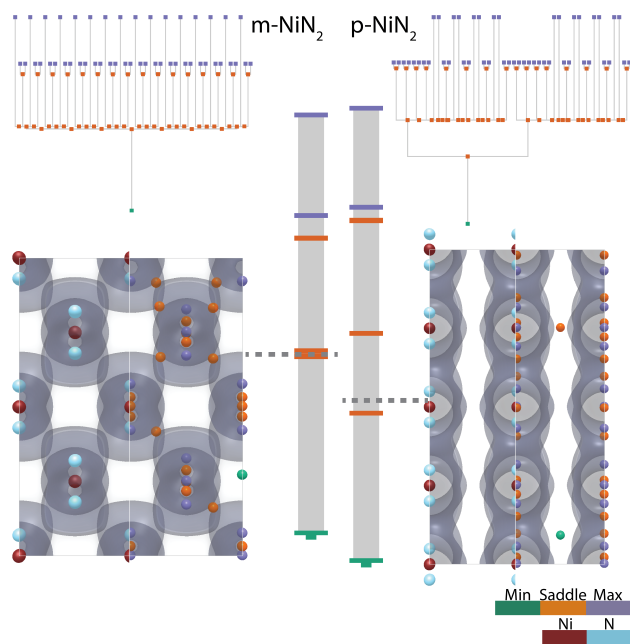
Figure 4: *m-NiN$_2$ and p-NiN$_2$ (38.0 GPa), using a logarithmic scale for the charge density. Full trees together with summary bars and spatial representations using an orthographic projection and showing the isosurfaces for the lowest saddle points together with atom and critical point positions. One can clearly see the layered structure in p-NiN$_2$.*

Figure 5: *Comparison of metal and alloy, using a logarithmic scale for the charge density. Full trees with summary bars and spatial representation using a perspective projection. The atoms and critical point positions are shown together with the isosurfaces (using the same isovalue for both, derived from a saddle point in the alloy). The summary bars give a quick overview showing difference between the symmetric metal and the distorted alloy.*

is indeed a layered material. For increasing pressures, these saddle values grow closer together, meaning that the merge from chains into layers and then into a single component happens almost simultaneously and the material does not have as clear separation into layers. For the highest pressure, 83.6 GPa, the layers cannot be distinguished, which is confirmed by the isosurface representations. This finding from our analysis has also been used in a physics publication by our collaboration partners [BFC*21].

A second example of a layered material is NiN$_2$, shown in Figure 4. The full trees can be seen together with the summary bars and isosurfaces for the lowest saddle points. Together with the isosurface we render the atom positions and critical point positions. One can clearly distinguish the layers in the p-NiN$_2$, while the m-NiN$_2$ has a different structure. This is also observed in the summary bars where the lowest saddle points for m-NiN$_2$ have similar values, meaning that the atoms merge into one volumetric structure at once, without forming any layers.

4.2. Comparing metal and alloy

In Figure 5 we show the full trees and the summary bars as well as selected isosurface representations, together with atom positions and critical point positions, for the metal and alloy data. The isovalue is based on one of the higher saddle points for the alloy tree, and for simplicity, we use the same isovalue for the metal. Both the tree and the summary bars highlight the difference in structure between the two materials; the Nb-metal is highly ordered and symmetric, while the alloy is distorted. This is seen in the spread in saddle points and maxima. The five different atom types in the
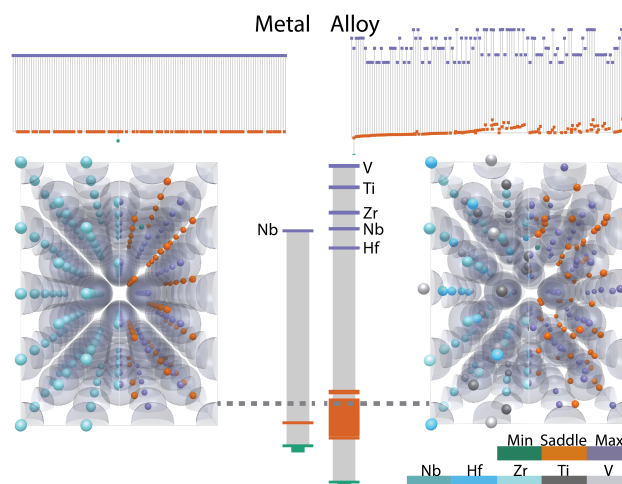
alloy can be observed in the summary bar as five distinct maximum values (the Nb atom still has a similar value as in the metal).

5. Discussion and Conclusions

We presented an approach that provides a quantitative and visual summary of important structures in charge density fields of materials based on a well-studied topological data structure, the merge tree. This summary can be expanded on demand to reveal finer levels of detail of the structures. We demonstrated how these methods can be utilized to compare different materials and quickly identify whether a particular structure, such as layers, is present or not. The method has been developed in close collaboration with the domain scientists, going through several iterations. The results sparked new ideas for further development of the method and its applications. For example, these methods can be very useful in the visual comparative analysis of ensembles and in observing the structural changes in ensemble members as one or more input parameters are changed. We believe the visualization of complete materials databases would also be possible. In terms of improvements to the analysis method, marrying the topological approach with meaningful geometric measures such as shape descriptors [SFL*21] would be one of our major directions for future research. Another interesting direction could be to explore the automatic identification of symmetric topological structures in merge trees [TN11].

References

[AMFH21] ABRIKOSOV A., MASOOD T. B., FALK M., HOTZ I.: Topological analysis of density fields: an evaluation of segmentation methods. *Computers & Graphics 98* (2021), 231–241. doi:10.1016/j.cag.2021.05.015. 1

[Bad85] BADER R. F. W.: Atoms in molecules. *Accounts of Chemical Research 18*, 1 (1985), 9–15. doi:10.1021/ar00109a003. 1, 2

[BB24] BERNAL J. D., BRAGG W. L.: The structure of graphite. *Proceedings of the Royal Society of London. Series A, Containing Papers of a Mathematical and Physical Character 106*, 740 (1924), 749–773. doi:10.1098/rspa.1924.0101. 1

[BBP*21] BYKOV M., BYKOVA E., PONOMAREVA A. V., TASNÁDI F., CHARITON S., PRAKAPENKA V. B., GLAZYRIN K., SMITH J. S., MAHMOOD M. F., ABRIKOSOV I. A., GONCHAROV A. F.: Realization of an ideal cairo tessellation in nickel diazenide NiN_2: High-pressure route to pentagonal 2d materials. *ACS Nano 15*, 8 (2021), 13539–13546. doi:10.1021/acsnano.1c04325. 2

[BFC*21] BYKOV M., FEDOTENKO T., CHARITON S., LANIEL D., GLAZYRIN K., HANFLAND M., SMITH J. S., PRAKAPENKA V. B., MAHMOOD M. F., GONCHAROV A. F., PONOMAREVA A. V., TASNÁDI F., ABRIKOSOV A. I., BIN MASOOD T., HOTZ I., RUDENKO A. N., KATSNELSON M. I., DUBROVINSKAIA N., DUBROVINSKY L., ABRIKOSOV I. A.: High-pressure synthesis of Dirac materials: layered van der Waals bonded BeN_4 polymorph. *Physical Review Letters 126*, 17 (2021), 175501. doi:10.1103/PhysRevLett.126.175501. 1, 2, 4

[BGL*18] BHATIA H., GYULASSY A. G., LORDI V., PASK J. E., PASCUCCI V., BREMER P.-T.: TopoMS: Comprehensive topological exploration for molecular and condensed-matter systems. *Journal of Computational Chemistry 39*, 16 (2018), 936–952. doi:https://doi.org/10.1002/jcc.25181. 1

[BOH11] BOSTOCK M., OGIEVETSKY V., HEER J.: D³ data-driven documents. *IEEE Transactions on Visualization and Computer Graphics 17*, 12 (2011), 2301–2309. doi:10.1109/TVCG.2011.185. 2

[CCK*14] CAFLISCH R. E., CEDER G., KREMER K., POLLOCK T., SCHEFFLER M., WANG E. G.: Focus on novel materials discovery. *New Journal of Physics 16* (2014). 1

[CSA03] CARR H., SNOEYINK J., AXEN U.: Computing contour trees in all dimensions. *Computational Geometry 24*, 2 (2003), 75–94. Special Issue on the Fourth CGC Workshop on Computational Geometry. doi:10.1016/S0925-7721(02)00093-7. 2

[CTOL*21] CASILLAS-TRUJILLO L., OSINGER B., LINDBLAD R., KARLSSON D., ABRIKOSOV A. I., FRITZE S., VON FIEANDT K., ALLING B., HOTZ I., JANSSON U., ABRIKOSOV I. A., LEWIN E.: Experimental and theoretical evidence of charge transfer in multicomponent alloys–how chemical interactions reduce atomic size mismatch. *Materials Chemistry Frontiers 5*, 15 (2021), 5746–5759. doi:10.1039/D1QM00380A. 1, 2

[GBCG*14] GÜNTHER D., BOTO R. A., CONTRERAS-GARCIA J., PIQUEMAL J.-P., TIERNY J.: Characterizing molecular interactions in chemical systems. *IEEE Transactions on Visualization and Computer Graphics 20*, 12 (2014), 2476–2485. doi:10.1109/TVCG.2014.2346403. 1

[GK10] GRAHAM M., KENNEDY J.: A survey of multiple tree visualisation. *Information Visualization 9*, 4 (2010), 235–252. doi:10.1057/ivs.2009.29. 1

[GKL*15] GYULASSY A. G., KNOLL A., LAU C., WANG B., BREMER P.-T., PAPKA M. E., CURTISS L., PASCUCCI V.: Morse-Smale analysis of ion diffusion in ab initio battery materials simulations. In *Topological Methods in Data Analysis and Visualization IV, Theory, Algorithms, and Applications*, Carr H., Garth C., Weinkauf T., (Eds.). Springer, 2015. doi:10.1007/978-3-319-44684-4_8. 1

[Gut20] GUTIÉRREZ H. R.: Two-dimensional layered materials offering expanded applications in flatland. *ACS Applied Nano Materials 3*, 7 (2020), 6134–6139. doi:10.1021/acsanm.0c01763. 1

[JKMS*10] JOHNSON E. R., KEINAN S., MORI-SÁNCHEZ P., CONTRERAS-GARCÍA J., COHEN A. J., YANG W.: Revealing noncovalent interactions. *Journal of the American Chemical Society 132*, 18 (2010), 6498–6506. doi:10.1021/ja100936w. 1

[JOH*13] JAIN A., ONG S. P., HAUTIER G., CHEN W., RICHARDS W. D., DACEK S., CHOLIA S., GUNTER D., SKINNER D., CEDER G., PERSSON K. A.: The Materials Project: A materials genome approach to accelerating materials innovation. *APL Materials 1*, 1 (2013), 011002. doi:10.1063/1.4812323. 1

[JSS*19] JÖNSSON D., STENETEG P., SUNDÉN E., ENGLUND R., KOTTRAVEL S., FALK M., YNNERMAN A., HOTZ I., ROPINSKI T.: Inviwo—a visualization system with usage abstraction levels. *IEEE Transactions on Visualization and Computer Graphics 26*, 11 (2019), 3241–3254. doi:10.1109/TVCG.2019.2920639. 2

[LTY*23] LANIEL D., TRYBEL F., YIN Y., FEDOTENKO T., KHANDARKHAEVA S., ASLANDUKOV A., APRILIS G., ABRIKOSOV A., MASOOD T. B., GIACOBBE C., BRIGHT E. L., GLAZYRIN K., HANFLAND M., WRIGHT J., HOTZ I., ABRIKOSOV I., DUBROVINSKY L., DUBROVINSKAIA N.: Aromatic Hexazine $[N_6]_4{}^-$ anion revealed in the complex structure of the high-pressure potassium nitrogen compound K_9N_{56}. *Nature Chemistry* (2023). to appear. 1

[LWL*20] LOHFINK A.-P., WETZELS F., LUKASCZYK J., WEBER G. H., GARTH C.: Fuzzy contour trees: Alignment and joint layout of multiple contour trees. *Computer Graphics Forum 39*, 3 (2020), 343–355. doi:10.1111/cgf.13985. 1

[SFL*21] SKÅNBERG R., FALK M., LINARES M., YNNERMAN A., HOTZ I.: Tracking internal frames of reference for consistent molecular distribution functions. *IEEE Transactions on Visualization and Computer Graphics 28*, 9 (2021), 3126–3137. doi:10.1109/TVCG.2021.3051632. 4

[SMH*22] SHEN J.-X., MUNRO J. M., HORTON M. K., HUCK P., DWARAKNATH S., PERSSON K. A.: A representation-independent electronic charge density database for crystalline materials. *Scientific Data 9*, 661 (2022). doi:10.1038/s41597-022-01746-z. 1

[TFL*17] TIERNY J., FAVELIER G., LEVINE J. A., GUEUNET C., MICHAUX M.: The Topology Toolkit. *IEEE Transactions on Visualization and Computer Graphics 24*, 1 (2017), 832–842. doi:10.1109/TVCG.2017.2743938. 2

[TN11] THOMAS D. M., NATARAJAN V.: Symmetry in scalar field topology. *IEEE Transactions on Visualization and Computer Graphics 17*, 12 (2011), 2035–2044. doi:10.1109/TVCG.2011.236. 4

[WDC*07] WEBER G. H., DILLARD S. E., CARR H., PASCUCCI V., HAMANN B.: Topology-controlled volume rendering. *IEEE Transactions on Visualization and Computer Graphics 13*, 2 (2007), 330–341. doi:10.1109/TVCG.2007.47. 2

[YMS*21] YAN L., MASOOD T. B., SRIDHARAMURTHY R., RASHEED F., NATARAJAN V., HOTZ I., WANG B.: Scalar field comparison with topological descriptors: Properties and applications for scientific visualization. *Computer Graphics Forum 40*, 3 (2021), 599–633. doi:https://doi.org/10.1111/cgf.14331. 1, 2